U.P.B. Sci. Bull., Series D, Vol. 69, No. 1, 2007 ISSN 1454-2358

ON THE AERODYNAMIC CHARACTERISTICS OF A CLASS OF AIRFOILS WITH CONTINUOUS CURVATURE AT SUBSONIC, TRANSONIC AND SUPERSONIC REGIMES

C. BERBENTE,[1] S. DĂNĂILĂ[2]

Lucrarea prezentă introduce o clasă de profile generate analitic, cu curbură continuă pe intrados şi pe extrados. În particular, se studiază aşa numitele „profile delfin", dar şi alte forme interesante pentru diverse regimuri de curgere sunt posibile. Ştiind că gradientul de presiune influenţează drastic evoluţia stratului limită, menţinerea unei curburi continue este importantă. Metoda utilizează funcţii spline polonomiale de ordinul trei. Rezultatele obţinute cu ajutorul codului FLUENT 6 pentru curgeri cu strat limită laminar şi turbulent sunt interpretate în raport de continuitatea curburii.

The present paper introduces a class of analytically generated aerodynamic profiles with continuous curvature on both upper and lower side. In particular, one studies a number of so called Dolphin profiles, but other shapes are also of interest for various flow regimes. Knowing the influence of the pressure gradient on the boundary layer flow, on one hand, and the influence of the airfoil shape on the pressure gradient distribution, on the other hand, maintaining the curvature continuity is important. The method is based on polynomial spline functions, with a degree of continuity up to second order derivative. In order to study the influence of the continuity of curvature radius on the aerodynamic characteristics, a systematic series of numerical test for two different Dolphin-type airfoils, with and without contiguous connection in curvature, respectively, were performed. The large amount of numerical results, generated by the FLUENT 6 code, is interpreted in respect to the continuity of curvature radius.

1. Introduction

It is well known that at supersonic speeds airfoils with sharp leading edges are adequate in order to create oblique low intensity shock waves and thus reduced drag coefficients. A series of analytical explicit third order formulas for such high speed inviscid regimes were established for example in the 60's by Carafoli and Berbente by using a unitary expression for pressure distribution in supersonic-hypersonic regime [1,2]. Recently, I. Ţăposu and his coworkers

[1] Professor, Department of Aerospace Sciences, "Elie Carafoli", University 'Politehnica" of Bucharest, ROMANIA
[2] Professor, Department of Aerospace Sciences, "Elie Carafoli", University "Politehnica" of Bucharest, ROMANIA

developed a theoretical (using inviscid models) and experimental study for a class of sharp leading edge airfoils –called "Dolphin"- [3,4,5] to be used even at subsonic speeds where thick round leading edge is usually recommended. The quoted authors report advantageous aerodynamic behaviors, experimentally confirmed at low speeds (hydrodynamic tunnel), as: delayed separation and maximum lift at angles of attack up to 25-30°. In these studies, parabola of second degree, connected in slope, generate the airfoil geometry. This yields to sudden jumps in radius of curvature in points of connection (two inflection points and the maximum thickness point, both on the upper and on the lower surface), impaired as instabilities sources, for example in incompressible flow calculations based on singularities distributions (sources, vortices, etc.).

In the follows we will try to improve the study of these Dolphin profiles at different flow regimes (subsonic, transonic and supersonic) checking out, simultaneously with the velocity field calculations, the influence of the airfoil geometry on the boundary layer flow. We will generate airfoil shapes without discontinuities on curvature radius and will give a special attention to the effect of curvature on the boundary layer evolution.

2. Airfoil geometry

The airfoil shape is generated by polynomial spline functions of third degree connected in four points. Lets be x_i, $i=0,\ldots,4$, a set of points on the profile chord, where $x_0=0$ and $x_4=c=1$ are the leading edge and the trailing edge, respectively; x_1 and x_3 are the inflection points and $x_2=k$ is the maximum thickness point (Fig.1). Supposing a symmetrical airfoil, only the upper surface will be considerate. Let's be y_i, $i=0,\ldots,4$ the corresponding ordinates of airfoil shape on the assumed set of chord points. So, we have:

$$x_0=0, y_0=0, x_2=k, y_2=\varepsilon,\ x_4=c=1, y_4=0. \tag{1}$$

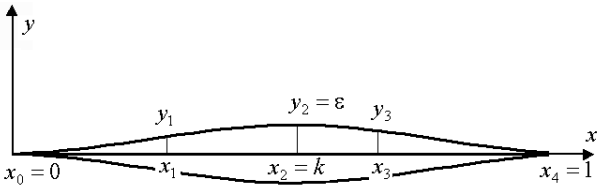

Fig. 1. Airfoil geometry

A contiguous shape up to second order derivative can be obtained by polynomial spline function at least third degree. Denoting by $p_{3i}(x)$ the restriction of the polynomial spline function on the interval $[x_i, x_{i+1}]$, we have [7]

$$p_{3i}(x) = y_i + m_i(x - x_i) + b_i(x - x_i)^2 + a_i(x - x_i)^3,\ x \in [x_i, x_{i+1}],\ i = 0,\ldots,3, \quad (2)$$

where m_i, a_i, b_i, $i = 0,\ldots,3$ are, up to now, unspecified coefficients. The m_i coefficients represent the point slopes and the b_i's are proportional to the point curvature radius.

The continuity conditions up to second order derivatives, including, yield to following relations [7]:

$$a_i h_i^3 = h_i(m_i + m_{i+1}) - 2(y_{i+1} - y_i),\ b_i h_i^2 = 3(y_{i+1} - y_i) - h_i(m_{i+1} + 2m_i), \quad (3)$$

$h_i = x_{i+1} - x_i$, $i = 0,\ldots,3$.

Slopes m_i are the solution of the system of equations:

$$\rho_i m_{i-1} + 2m_i + \lambda_i m_{i+1} = d_i,\ i = 1,\ldots,3, \quad (4a)$$

where

$$\rho_i = \frac{h_i}{h_{i-1} + h_i},\ \lambda_i = \frac{h_{i-1}}{h_{i-1} + h_i},\ d_i = 3\left(\frac{\lambda_i}{h_i}(y_{i+1} - y_i) + \frac{\rho_i}{h_{i-1}}(y_i - y_{i-1})\right), \quad (4b)$$

$$h_i \neq 0,$$

Usually, the coordinates $(x_i, y_i), i = 0,\ldots,4$, together with the slopes on the boundary points (m_0 and m_4, respectively) are given and the problem is entirely determined (all coefficients m_i, a_i, b_i, $i = 0,\ldots,3$, are known). However, in the present analysis, we are interested to keep as parameters, for example, the inflection point positions, x_1, x_3, and the maximum thickness position, k. Accordingly to the definition of Dolphin profile we'll assume zero slopes at both leading and trailing edges:

$$m_0 = m_4 = 0. \quad (5)$$

Consequently to the definition of inflections and maxims, we have:

$$y_1'' = 0,\ y_2' = 0,\ y_3'' = 0 \quad (6)$$

Imposing conditions (6) for the polynomials (2) yield:

$$b_1 = 0,\ m_2 = 0,\ b_3 = 0. \quad (7)$$

On the other hand, the maximum thickness, $y_2 = \varepsilon$ have to be given, five parameters: x_1, y_1, x_2, x_3, y_3, remain to be determined from three equations (7). Therefore, two independent parameters remain. Through the possible chooses are

the pairs: a) (x_1, x_2), positions of the first inflection and the maximum thickness points; b) (x_1, x_3), positions of inflection points; c) (y_1, y_3) with $y_1 < \varepsilon$, $y_3 < \varepsilon$, the thickness airfoil in the inflection points, etc.

Taking into account conditions (5), (6), as solution of system (4) yields:

$$m_1 = \frac{d_1}{2},\ m_3 = \frac{d_3}{2},\ 2d_2 - \rho_2 d_1 = \lambda_2 d_3 \tag{8}$$

Replacing:

$$h_0 = x_1,\ h_1 = k - x_1,\ h_2 = x_3 - k,\ h_3 = 1 - x_3, \tag{9}$$

the following expressions result:

$$\rho_1 = 1 - \frac{x_1}{k};\ \lambda_1 = \frac{x_1}{k},\ \rho_2 = 1 - \frac{x_3 - k}{x_3 - x_1},\ \lambda_2 = \frac{k - x_1}{x_3 - x_1};\ \rho_3 = \frac{1 - x_3}{1 - k},$$
$$\lambda_3 = \frac{x_3 - k}{1 - k} \tag{10a}$$

$$\frac{d_1}{3} = \frac{x_1}{k}\frac{\varepsilon - y_1}{k - x_1} + \frac{k - x_1}{k x_1} y_1,\ \frac{d_2}{3} = \frac{k - x_1}{x_3 - x_1}\frac{y_3 - \varepsilon}{x_3 - k} + \frac{x_3 - k}{x_3 - x_1}\frac{\varepsilon - y_1}{k - x_1},$$
$$\frac{d_3}{3} = \frac{x_3 - k}{1 - k}\frac{(-y_3)}{1 - x_3} + \frac{1 - x_3}{1 - k}\frac{y_3 - \varepsilon}{x_3 - k}. \tag{10b}$$

Canceling the coefficients b_1 and b_3, from (7) yield:

$$b_1 = 0,\ (\varepsilon - y_1) - \frac{1}{3} d_1 (k - x_1) = 0, \tag{11a}$$

$$b_3 = 0,\ -y_3 - \frac{1}{3} d_3 (1 - x_3) = 0, \tag{11b}$$

or:

$$\frac{d_1}{3} = \frac{\varepsilon - y_1}{k - x_1},\ \frac{d_3}{3} = \frac{-y_3}{1 - x_3}. \tag{12}$$

Finally, for the parameters x_1, y_1, k, x_3, y_3, the following three relations, deduced from (12) and (8), result:

$$(1 - \frac{x_1}{k})\frac{\varepsilon - y_1}{k - x_1} = \frac{k - x_1}{k x_1} y_1;\ y_1 = \frac{\varepsilon}{k} x_1 = \frac{x_1}{k}\varepsilon \tag{13}$$

$$\frac{1-x_3}{1-k}\frac{\varepsilon-y_3}{x_3-k}=\frac{y_3}{1-x_3}\frac{1-x_3}{1-k},\ y_3=\frac{1-x_3}{1-k}\varepsilon \tag{14}$$

$$\frac{y_3}{\varepsilon}=\frac{2-k-x_3}{1-x_3}=2-\left(\frac{x_3-k}{k-x_1}\right)^2\left(1-\frac{y_1}{\varepsilon}\right). \tag{15}$$

From equations (13) and (14) and (15), we obtain the solutions:

$$x_3=k,\ \frac{x_3}{k}=\frac{1-x_1}{1-k} \tag{16}$$

and evidently, only the second has signification.

Now, the slops m_1 and m_3 can be calculated. So, from (12) we obtain:

$$\frac{d_1}{3}=\frac{\varepsilon}{k};\ m_1=\frac{3}{2}\frac{\varepsilon}{k};\ \frac{d_3}{3}=-\frac{\varepsilon}{1-k};\ m_3=\frac{-3}{2}\frac{\varepsilon}{1-k}. \tag{17}$$

It is interesting to calculate the curvature radius at lading and trailing edges, respectively:

$$R_0=\frac{(1+y_0'^2)^{3/2}}{y_0''}=\frac{1}{2b_0}=\frac{kx_1}{2\varepsilon};\ R_4=\frac{(1-k)(1-x_3)}{2\varepsilon}. \tag{18}$$

The coefficients $a_i,\ b_i,\ i=0,\ldots,3$, have next expressions:

$$a_0x_1^2=a_1(k-x_1)^2=-\frac{\varepsilon}{2k};\ a_2(x_3-k)^2=a_3(1-x_3)^2=\frac{\varepsilon}{2(1-k)}, \tag{19a}$$

$$b_0x_1=\frac{3\varepsilon}{2k};\ b_1=b_3=0;\ b_2(x_3-k)=-\frac{2\varepsilon}{2(1-k)}. \tag{19b}$$

In this way the airfoil shape is entirely determinate. Although, theoretically, we have two free parameters on dispose, however, the expressions of coefficients $m_i,\ b_i,\ a_i,\ i=0,\ldots,3$, depend mainly on the position k of the maximum thickness. That suggests a weak flexibility than expected in variation of inflection points positions x_1 and x_3.

In order to study the effect of continuity on curvature radius, we assume as reference the airfoil shape generated by point connected parabola arcs. Let's be $p_{2i}(x)$ the restriction of the second order polynomial spline function on interval $[x_i, x_{i+1}]$:

$$p_{2,i}(x)=y_i+m_i(x-x_i)+b_i(x-x_i)^2,\ x\in[x_i,x_{i+1}],\ i=0,\ldots,3. \tag{20}$$

Imposing the continuity in values and slops on intermediate points, yield:

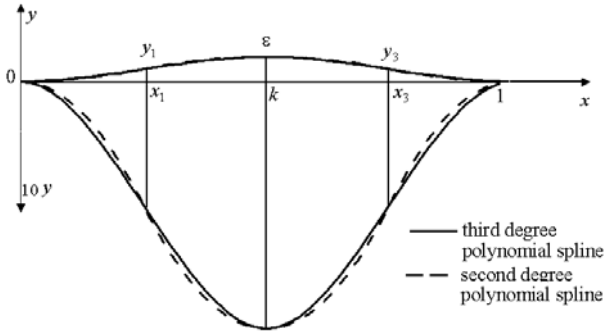

Fig,2. Airfoil generated by polynomial spline functions

$$p_{2,i}(x_{i+1}) = p_{2,i+1}(x_{i+1})\,;\ p'_{2,i}(x_{i+1}) = p'_{2,i+1}(x_{i+1})\,, \tag{21}$$

or:

$$y_i + m_i(x_{i+1} - x_i) + b_i(x_{i+1} - x_i)^2 = y_{i+1}\,;\ m_i + 2b_i(x_{i+1} - x_i) = m_{i+1} \tag{22}$$

Solving the above system of equations, we obtain:

$$b_i = \frac{1}{2h_i}(m_{i+1} - m_i)\,,\ m_{i+1} + m_i = \frac{1}{2h_i}(y_{i+1} - y_i)\,, \tag{23}$$

where $h_i = x_{i+1} - x_i$. Taking as parameters inflection points positions x_1, x_3 and the maximum thickness position, $x_2 = k$, for $m_0 = m_2 = m_4 = 0$, we obtain:

$$m_1 = \frac{2\varepsilon}{k}\,;\ m_3 = -\frac{2\varepsilon}{1-k} \tag{24}$$

and the airfoil coordinates at inflections are:

$$\begin{gathered} y_1 = \frac{x_1}{k}\varepsilon\,;\ y_3 = \frac{1-x_3}{1-k}\varepsilon\,.\ b_0 = \frac{\varepsilon}{x_1 k}\,; \\ b_1 = -\frac{\varepsilon}{k(k-x_1)}\,; b_2 = \frac{\varepsilon}{(x_3-k)(k-1)}\,; b_3 = \frac{\varepsilon}{(x_3-1)(k-1)} \end{gathered} \tag{25}$$

together with the b_i coefficients (25).

Fig. 2 (upper side) plots the resulting airfoils for $2\varepsilon = 0.1$, $x_1 = 0.25$, $k = 0.5$. Solid line corresponds to the Dolphin airfoil generated by third degree polynomial spline function (D3DPS) and dashed line represents the airfoil obtained by second-degree polynomial connected arcs (D2DPS). On the same plot, in lower side, to make visible differences between the shapes, the transverse coordinate is multiplied by a factor of 10. On the neighborhood of the sharp

landing edge, the positive slope dy/dx of the D3DPS-airfoil is larger than the corresponding slope of D2DPS-airfoil. In the vicinity of the maximum thickness, initially, on the ascending branch the slope of D2DPS-airfoil exceeds the slope of the D3DPS-airfoils. For $x > k$, the relation between slopes of the two analyzed profiles is reversed.

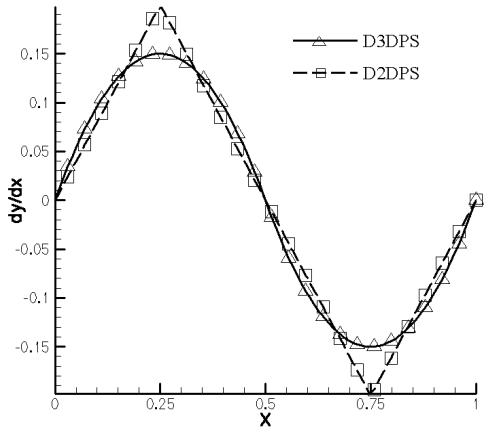

Fig. 3 Slope distribution

That suggests, for D3DPS-airfoils, at-least in incompressible flows, a grater negative (favorable) pressure gradient, and a smaller positive (adverse) pressure gradient, with respect to D2DPS airfoil. Knowing the influence of the pressure gradient on the development of boundary layer flow, we expect an improving of the aerodynamic characteristic for airfoils with contiguous curvature radius.

3. Numerical aspects

To compare airfoils generated by third degree polynomial spline function (D3DPS) with airfoil generate by second-degree polynomial connected arcs (D2DPS), a series of computational tests was carried out using FLUENT 6 code. For numerical experiments, the D3DPS and D2DPS airfoils with 10% thickness ratio were chosen. Also, the other geometric elements involved in airfoils geometry creation were taken identically for both airfoils: $x_1 = 0.25$, $k = 0.5$, $x_3 = 0.75$. . In order to obtain accurate information on influence of curvature radius continuity on the aerodynamic characteristics, the numerical results were obtained on the same computational mesh (only the solid surface was changed accordingly to the airfoil shape).

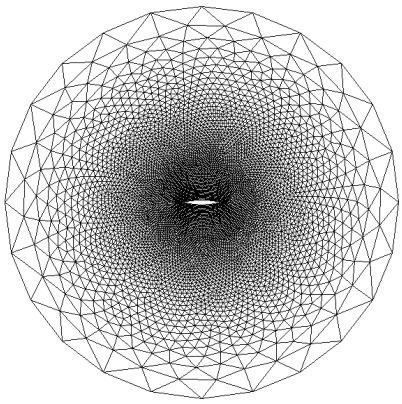

Fig.4. Computational grid for inviscid flows.

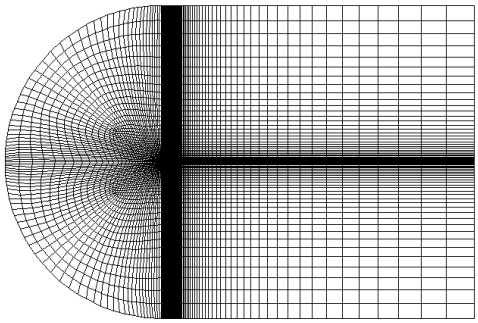

Fig.5. Computational grid for viscous flows.

For in viscid flow calculations an unstructured triangular mesh with 11270 cells and 16957 interfaces was build (fig.4), imposing 40 equidistant points on airfoils surface (20 on the upper surface and 20 on the lower surface, respectively). The radius of the external circular boundary was assumed to be about 5 times the profile chord.

For viscous cases, the computational the structured computational grid is presented in fig.5 (12350 cells, 24960 interfaces). A number of double sided refined 100 points, on the solid profile surface was employed (50 on the upper surface and 50 on the lower surface, respectively). The computational domain was extended about 15 chord lengths upstream and about 30 chord lengths downstream. On the vicinity of both, upper and lower airfoil surfaces, boundary layer zones were included.

4. Inviscid flow model results

Fig. 6 presents the incompressible pressure distribution at zero angle of attack. As expected, the influence of curvature radius is reflected in the slope of pressure distribution on the airfoil. Moreover, the pressure coefficient peaks reached on the D2DPS overrides the corresponding value of D3DPS-profile.

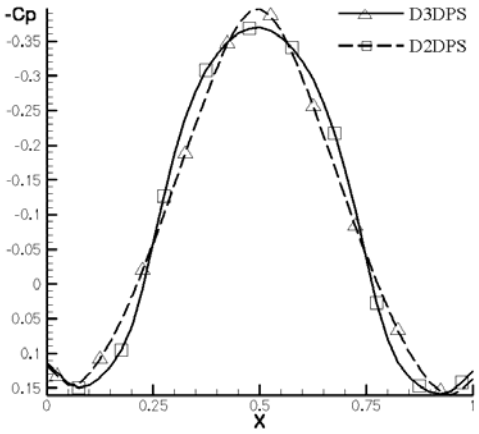

Fig. 6. Incompressible pressure distribution, $\alpha = 0$.

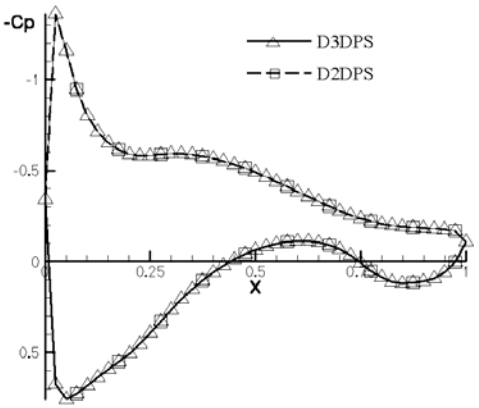

Fig. 7. Incompressible pressure distribution, $\alpha = 10^{\circ}$.

At nonzero incidence (fig.7), both airfoils produce the same pressure distribution, due the identical camber of mean line, as already knowing from the linear airfoil theory. For transonic flow, the obtained numerical results are plotted in fig. 8 and 10, for M=0.85 and incidence, $\alpha = 0$. Although the shock location is indifferent at curvature radius continuity, a diminishing in intensity shock wave for the D3DPS airfoil is present (fig.8). Fig. 10 plots the pressure contours around the D3DPS airfoil at zero incidences. The shock wave "thickness" observed in figure is specific to all first order upwind Euler solvers.

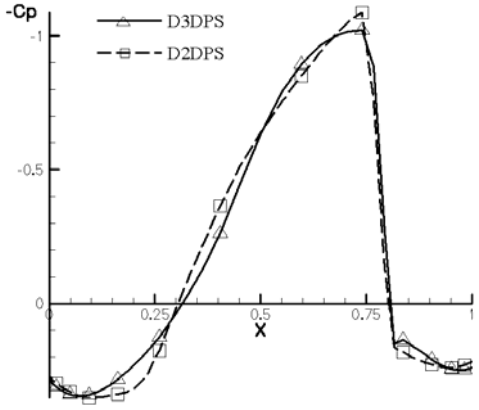

Fig. 8. Inviscid flow, M=0.85, $\alpha = 0$.

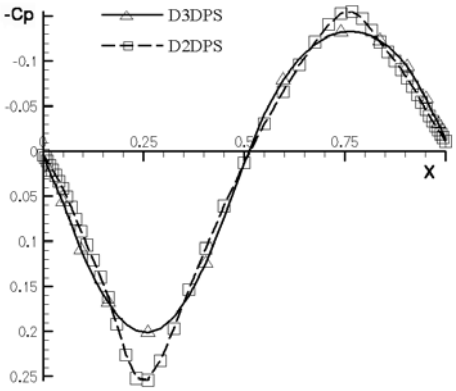

Fig. 9. Inviscid flow, M=2, $\alpha = 0$

Fig. 9 and 11 present the pressure distribution and Mach contours, respectively, at M=2 and incidence, $\alpha = 0^{\circ}$. Again, the pressure gradient and the extreme values of pressure coefficient are higher on the D2DPS airfoil.

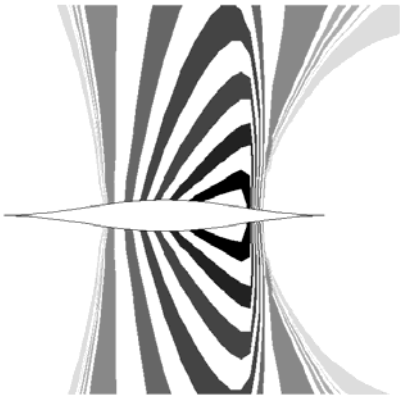

Fig. 10 Pressure contours for D3DPS, M=0.85, $\alpha = 0^\circ$

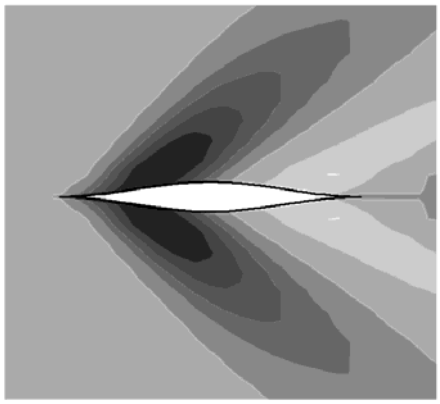

Fig. 11 Mach contours for D3DPS, M=0.85, $\alpha = 0^\circ$

5. Constant viscosity fluid flow (laminar flow)

The obtained results for the constant viscosity fluid flow (laminar flow) are presented in fig. 12-14. These plots are similar to those presented for inviscid fluid flow. In fig.15 we represent the skin friction coefficient distribution on the solid airfoil surfaces at M=0.85 and zero incidence. The continuity of the curvature radius influences the friction coefficient only upstream of shock wave. The calculated aerodynamic drag coefficients at zero angle of attack for D3DPS airfoil are: $C_D = 0.01732$ at incompressible flow, and $C_D = 0.06128$ at M=0.85. For D2DPS airfoil the corresponding values are $C_D = 0.01936$ in incompressible flow and $C_D = 0.06603$ at M=0.85. We observe a diminution of about 10% in drag coefficient value due the continuity of curvature radius.

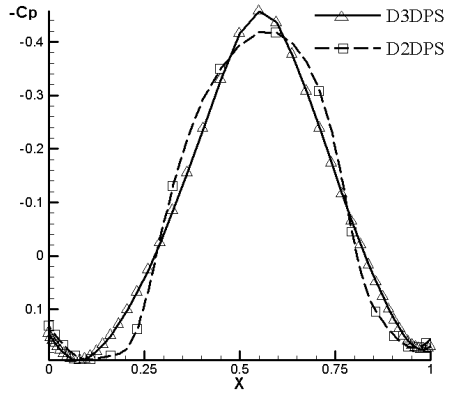

Fig.12. Pressure distribution, incompressible laminar flow $\alpha = 0^\circ$

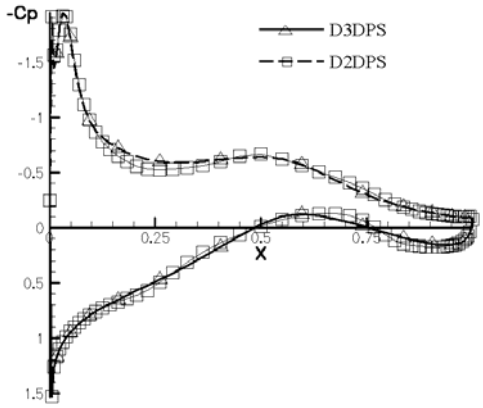

Fig.13 Pressure distribution, incompressible laminar flow, $\alpha = 10^\circ$

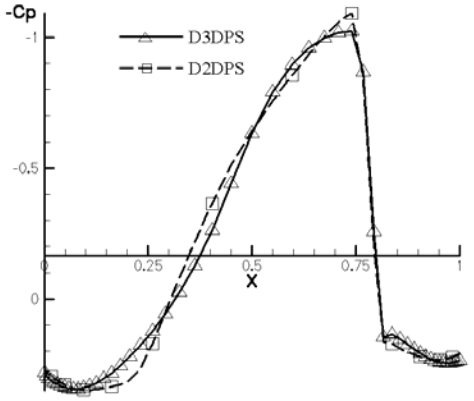

Fig.14. Pressure distribution, laminar flow, M=0.85, $\alpha = 0^{\circ}$

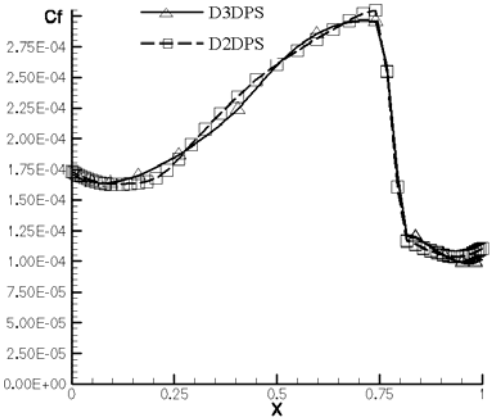

Fig.15 Skin friction coefficient distribution laminar flow, M=0.85, $\alpha = 0^{\circ}$

6. Turbulent flow

For turbulent flow calculations, the standard $k-\varepsilon$ turbulence model was adopted, combined with wall function formulation of boundary conditions. Therefore, the distance to the wall of first row grid points was calibrated each time to obtain a value of about 40 for the dimensionless parameter y^+ [8].

Table 1 presents the global aerodynamic coefficients as function of incidence at different Mach numbers. From the above data one can conclude the positive effect of the radius continuity on the drag coefficient, C_D, at low incidences (0°–2°): a diminution of C_D for 3DPS airfoil as compared to the 2DPS airfoil up to 9 % in the range of such small angles of attack corresponding to the cruise regimes for commercial airliners of large speeds. At M=2 and α = 0, one gets a 19% diminution in C_D at turbulent flow.

Table 1

		D3DPS			D2DPS		
M	α [deg]	C_D	C_L	C_M	C_D	C_L	C_M
0	0	0.023975	0	0	0.026041	0	0
	10	0.15583	0.8159	0.23659	0.1587	0.82074	0.23980
	20	0.4411	1.1466	0.409990	0.4433	1.1467	0.41216
0.85	0	0.064911	0	0	0.066239	0	0
	10	0.2778	1.29066	0.55293	0.2767	1.1979	0.53599
	20	0.6912	1.78277	0.80345	0.68999	1.7741	0.79808
1.2	0	0.030861	0	0	0.03813	0	0
	10	0.1071	0.4183	0.19293	0.1101	0.4201	0.19406
	20	0.3743	0.900	0.39445	0.3759	0.899	0.39415
2	0	0.030861	0	0	0.033813	0	0
	2	0.033616	0.082066	0.037259	0.036619	0.082101	0.037326
	10	0.069648	0.392170	0.192930	0.069531	0.391221	0.194060
	20	0.291470	0.929053	0.394450	0.289810	0.929158	0.394150

In Table 2, a comparison between the analytical Carafoli- Berbente inviscid formulas, C_{LA} , C_{DA} and Fluent 6, C_{LF} , C_{DF} for the lift and drag coefficients is given, at Mach number M=2 and various angles of attack. The agreement especially at non zero angles of attack is surprisingly good.

Table 2

Comparison between the analytical inviscid formulas (Carafoli-Berbente) and Fluent 6

M	α (deg)	C_{DF}	C_{DA}	*Error* %	C_{LF}	C_{LA}	*Error* %
2	0	0.030861	0,028523	8.85	0	0	0
	10	0.1071	0.106321	0.724	0.4183	0.42900	–2.56
	20	0.3743	0.36748	1.84	0.900	0.90935	–1.09

7. Conclusions

The main effect of the continuity of curvature radius is the smooth variation of pressure gradient on the airfoil surface. This effect is benefic for the pressure drag and also for the boundary layer development. Compared with an airfoil without continuity on curvature radius, the drag reduction is about 9%, at moderate angle of attack.

Acknowledgement

This paper has received the support of Romanian.Space Agency and of Ministry of Education and Research within the Project Nr.142/2004-*"Models and modern numerical and experimental solutions regarding the flows around aerodynamical configuratins of practical interest"*.

REFERENCES

[1] *Carafoli E., Berbente C.,* Caracteristicile aerodinamice ale profilelor în regim supersonic-hipersonic, în cazul neglijării pierderilor de sarcină datorită undelor de şoc, SCMA, No.4, 1963.

[2] *Carafoli E., Berbente C.,* Determination of the Characteristics of Aerodynamic Profiles in Supersonic-Hypersonic Flow, Considering The pressure Losses Through Shock Waves, Rev. Roum. Sci. Techn, Mec. Appl, Tom 5, 1964.
[3] *Tăposu, I.* Dolphin Profiles, a New Concept in Aerodynamics (in Romanian), Ed, Tehnică, Bucureşti, 2002.
[4] *Ţăposu, I., Spătaru, P.,* About the Experimental Results of Dolphin Profile at Low Speeds, AIAA Applied Aerodynamics Conference, TP 2000-4506, Denver, Colorado, 2000
[5] *Obreja, D., Iorga*, *GH*., Experimental Results in Water Tunnel for a Naval Rudder, (in Romanian), Rapp. Ae. 4469, ICEPRONAV Galaţi, 2001.
[6] *Berbente, C., Mitran*, *S., Zancu, S.,* Numerical Methods, (in Romanian), Ed. Tehnică, Bucharest, 1997.
[7] *Dănăilă, S., Berbente, C.,* Numerical Methods in Fluid Dynamics, (in Romanian), Ed. Academiei, Bucharest, 2003.